Simulations and measurements of the performance of a channeled neutron guide for a time-of-flight spectrometer at the NIST Center for Neutron Research

Jeremy C. Cook[a)]
Department of Materials Science and Engineering, University of Maryland, College Park, Maryland 20742-2115 and NIST Center for Neutron Research, National Institute of Standards and Technology, 100 Bureau Drive, Stop 8563, Gaithersburg, Maryland 20899-8563

John R. D. Copley
NIST Center for Neutron Research, National Institute of Standards and Technology, 100 Bureau Drive, Stop 8562, Gaithersburg, Maryland 20899-8562

(Received 12 May 2003; accepted 10 November 2003)

We describe the identification and analysis of the principal sources of intensity loss within the five-channeled neutron guide tube that was originally installed in the chopper section of the Disk Chopper Spectrometer at the National Institute of Standards and Technology Center for Neutron Research. (The purpose of the five channels was to optimize intensity and resolution in three different modes of operation known as ''resolution modes.'') By combining measurements, Monte Carlo simulations, and analytical calculations, we have developed a model that successfully explains performance losses in the original guide. We have used this model to quantify expected returns in performance using a replacement guide in which the principal contributions to the intensity loss are reduced to the minimum achievable with current technology. We have also estimated the intensity gains that would be achieved if one of the limited number of options were adopted for modifying the original guide in a manner likely to produce such gains. We describe factors that affect the performance of the original guide and compare the measured and predicted performance of the modified guide against predictions for the optimal replacement guide. The simulations indicate that the modified guide (which has three channels rather than the original five) produces greater intensity gains over a large incident wavelength band for the low and medium resolution modes, whereas a high quality replacement guide greatly improves performance in the high resolution mode of operation. Because the low and medium resolution modes are most heavily demanded, we opted to modify the guide rather than replace it. We describe the nature of this modification and present intensity measurements that meet or exceed predictions in all resolution modes with no detectable change in the energy resolution nor increase in the instrumental background. [DOI: 10.1063/1.1638871]

I. INTRODUCTION

The Disk Chopper Spectrometer (DCS)[1] at the National Institute of Standards and Technology (NIST) Center for Neutron Research (NCNR) is classified as a direct-geometry neutron time-of-flight spectrometer. Such spectrometers use nominally monoenergetic (or fixed neutron wavelength) incident beams. On the DCS, the incident wavelength bandwidth is defined by two pairs of counterrotating chopper disks,[2,3] one at the extreme upstream end of the chopper system (referred to as the ''pulsing'' disk pair) and the other at the extreme downstream end of the chopper system (the ''monochromating'' disk pair). The disks of each pair have three slots of different width. Either the wide, the medium, or the narrow slots can be chosen to transmit the beam by choosing the relative phasing of the disk pairs appropriately. This enables the incident neutron energy resolution to be selected from one of three values for each incident wavelength without changing the chopper disk speed. Actually, the slots on the pulsing disk pair are wider than the corresponding slots on the monochromating disk pair. This is deliberate and produces a better compromise between intensity and elastic energy resolution than equal width slots on both pairs.[4,5] Use of the wide, medium, or narrow slot sets on the DCS is referred to as running in low, medium, or high resolution mode, respectively. Typically the required elastic resolution $\delta E_{\mathrm{el}}/E$ is better than 5% for experiments using this type of spectrometer. In order to obtain this resolution and maintain a useful beam size, the DCS has a large separation ($\approx$9 m) between the pulsing and monochromating chopper pairs despite the high maximum rotation frequency of the disks (333 Hz).

If neutron beams were perfectly collimated, transporting them over the large separations between the disks would present no problem. However, for beams emanating from long guides, the beam divergence is typically 1.7 mrad per angström neutron wavelength or greater, depending on which type of reflective coating is used in the guide. The DCS

a)Author to whom correspondence should be addressed; electronic mail: jeremy.cook@nist.gov

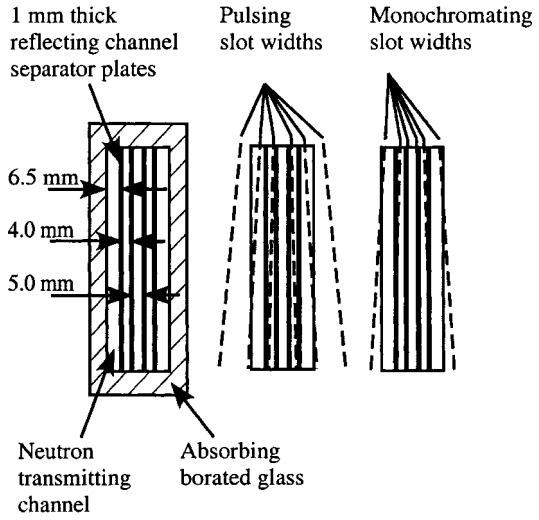

FIG. 1. Schematic cross-sectional view of the original guide arrangement showing the five channels that are created by introducing four channel separators. The nominal widths of the channels are indicated (the channels are nominally symmetric about a vertical bisector). The angular extent of the wide, medium, and narrow slot sets on the first (pulsing) and last (monochromating) counterrotating chopper disk pairs is also shown as they would appear when fully open to the chopper guide and perfectly phased.

guide has side wall coatings that allow about 2 mrad/Å horizontal divergence and the top and bottom coatings allow about 3.4 mrad/Å vertical divergence. Considering the chopper separation, the beam width (not exceeding 30 mm), and the operating wavelength range of approximately 1.5–12 Å, we conclude that a beam ''concentrator'' is necessary to limit intensity losses due to beam divergence between the chopper disks. In the case of the DCS, the beam concentrator is a channeled neutron guide (Fig. 1).

The clearance in the grooves that receive the reflecting plates that separate the channels permits transverse movement of the plates and consequently reduces their parallelism. Angular misalignments are usually tolerable when the accumulated deviations that they impose on the neutron trajectory are small compared to the critical angle. Allenspach *et al.*[6] have investigated the effects of misalignments, including substrate waviness for a straight ''$m=2$'' supermirror guide ($m=2$ means that the supermirror has a critical angle twice that of natural Ni). For typical dimensions (40 m long, 50 mm wide, and 150 mm high with 0.5 m long sections), they show that negligible losses are incurred when the surface waviness (defined as the standard deviation of the distribution of the surface normals to the ideal direction) is less than 10^{-4} rad for the wavelength range from about 1 to about 10 Å. This agrees with acceptable flatness tolerances suggested by Samuel *et al.*[7] Allenspach *et al.* also suggested that losses due to transverse displacements or dimension errors of the guide are roughly proportional to the total offset area divided by the cross-sectional area of the guide. Lee and Klose[8] have also discussed such losses in the context of a more complex guide design that includes a neutron bender. For an approximately 17.5 m long guide composed of 0.5 m long sections with minimum internal dimensions of 25 mm (excluding the channels of the bender section), they found that random ''zigzag-type'' misalignments of between $\pm 0.075°$ ($\pm 1.3\times 10^{-3}$ rad) produce about a 3%–5% transmission loss for neutron wavelengths between 2 and 10 Å. Factors that affect the optimal channel width for the case of the bender are also discussed. In the case of the DCS channeled guide, the horizontal dimensions of the channels are a few mm rather than a few cm and the length of the individual glass plates is only 0.25 m or less. These factors are expected to impose even stricter tolerance on the alignment of the channels.

In this article, we assess the severity of losses due to misalignments and imperfect reflectivity in the DCS channeled guide. We describe the original guide and compare the measured beam intensity with simulation results for a channeled guide that is very well aligned and incorporates reflectivity models that are consistent with the best quality reflective coatings available. We have developed a simplified model for the misaligned guide which we have used to compare the cost-effectiveness of purchasing a replacement guide with an improved channel alignment and best-available reflective coatings against an alternative, inexpensive option in which the existing channeled guide is modified rather than replaced. We discuss why we have opted for the latter solution and show that the misaligned guide model is rather successful in predicting the measured intensity gain factors.

II. DESCRIPTION OF THE CHANNELED CHOPPER GUIDE

In order to maximize intensity, optimization of the guide width with respect to the chopper slot width is important.[5] While this may be achieved with a guide whose width is varied when changing the slot widths, the five-channeled chopper guide, whose cross section is shown schematically in Fig. 1, potentially achieves this goal for the three slot sets on the DCS choppers without having to adjust the guide width. Optimization of the channel widths depends on *a priori* assumptions about the reflection efficiency of the channel walls. The channel widths shown in Fig. 1 were selected on the basis of typical properties of conventional nonchanneled guides. Because the channel separators have nonzero thickness, the convenience of the channeled guide concept comes at the expense of some loss of beam area. In the real device, the channel separators are 1 mm thick, unpolished float glass plates coated with ''^{58}Ni-equivalent'' reflective coatings ($m \approx 1.2$ made from Ti–Ni bilayers), so-called because the critical angle for total reflection is similar to that of the ^{58}Ni isotope (about 2 mrad Å^{-1}). Each of the four separators is fabricated from 47 separate plates, each between 32 and 250 mm long, the majority being 250 mm long. In the present case, the thin channel separator plates are inserted (unglued) into grooves machined into thick upper and lower glass plates (known as rules). Because they are not glued, the separator plates are generally somewhat misaligned. The thick glass side walls of the guide, like the rules, are made from borated float glass with superpolished inner surfaces. The superpolishing technique is described in Ref. 7. The inner surfaces of the side walls have similar ^{58}Ni-equivalent coatings to those used on the separator plates. The inner surfaces

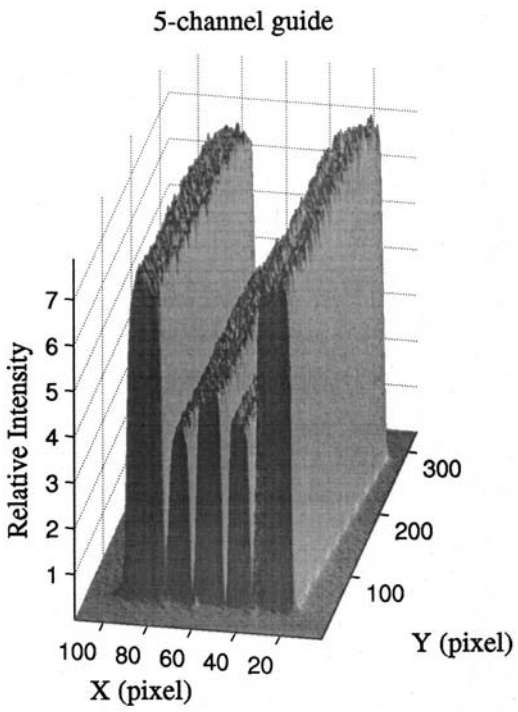

FIG. 2. Measured spatial distribution of neutron flux at the end of the channeled guide with the choppers removed (white beam). For the Dy foil used in this measurement, the pixel intensities are roughly proportional to the capture flux, not the integral flux.

of the rules (between the grooves) are coated with $m=2$ supermirror. The inner surfaces of the side walls are separated by 30 mm and the inner surfaces of the rules have 100 mm separation so that the maximum beam envelope is 30 mm wide$\times$100 mm tall. The reflectivities of the coatings are discussed further in Sec. IV. The original design has two outer channels of 6.5 mm nominal width, two intermediate channels of 4 mm nominal width, and a center channel of 5 mm nominal width (see Fig. 1). To good approximation, the widest monochromating chopper slots, when fully open, view all five channels, the intermediate width slots view the three inner channels, and the narrowest slots view only the center channel.

III. INITIAL FLUX MEASUREMENTS

For brevity, we loosely use the term ''flux'' (usually applied to particle fields) to refer to the neutron current density or fluence rate of the highly collimated neutron beam that crosses a plane that is normal to the beam direction. After commissioning of the DCS, the observed beam fluxes downstream of the channeled guide were appreciably lower than indicated by simulation results (described later in Sec. VI B) for the idealized five-channel guide. The dysprosium foil neutron radiograph[9] shown in Fig. 2, measured at the downstream end of the channeled guide with the choppers removed, revealed important channel flux differences marked by increasing attenuation with a decrease in channel width. The symmetry of the pattern also suggests that the attenuation is characterized by quantities related to the channel width, the mean number of reflections required for neutron transmission down the channel, for instance.

Further flux measurements were performed including gold foil activation measurements[10] which yielded capture flux values (i) upstream of the chopper system (white beam), (ii) downstream of the chopper system using a white beam (choppers stopped with their slots positioned to transmit the beam), and (iii) downstream of the chopper system using a ''monochromatic'' beam (choppers spinning and phased for various wavelengths). These last results were used to calibrate the primary beam monitor count rates so that absolute beam fluxes could be obtained for many wavelengths and for all three resolution modes.

These combined measurements formed the basis of comparison by which the channeled guide model parameters (described in Sec. IV) were refined.

IV. CHANNELED GUIDE MODEL

With the original guide installed and operational, it was no longer possible to verify displacements, thicknesses, waviness, and individual reflectivities of the 188 individual glass plates that constituted the channel separators. We therefore developed a model of the guide to assess the influence of both the misalignments of the reflecting surfaces and the reflectivity of the coatings on the transmission efficiency in an effort to explain the flux measurements and better characterize the guide. We discuss each in turn.

Original specifications of the channel plates indicate that their thickness can vary between 0.9 and 1 mm and that their waviness is less than 10^{-4} rad. Lacking specific information on the original tolerances on the groove widths, we conclude that the maximum transverse displacement (or groove–plate clearance), $\delta_{\max}$, is greater than 0.1 mm but no more than 0.3 mm. The sides and rules of each guide section (typically about 0.75 m long) are parallel to within 10^{-4} rad. Using our in-house techniques, alignment with respect to the sides and rules to about 2.5×10^{-5} rad accuracy is possible, so it is reasonable to assume that the guide sections are aligned to about 10^{-4} rad or less. We also assume that the grooves are parallel with the side walls to within 10^{-4} rad. Consequently, the outer walls of the guide and the grooves are aligned within acceptable angular tolerances, defined in Refs. 6 and 8, but the channel plates may be misaligned by up to about 10^{-3} rad in the horizontal plane and two to three times this in the vertical. Even though the maximum vertical misalignments of the plates may be larger than the horizontal, their detrimental effect on the guide transmission is small compared to the horizontal misalignments. This was verified by preliminary Monte Carlo simulations and a simple justification is given in the Appendix.

The channel plates were not used as reference surfaces for the guide alignment, so it is reasonable to assume that they have misalignments that are independent of each other. Because the effect of the vertical misalignments of the plates is small compared to the horizontal, we consider only horizontal misalignments. The (horizontal) angular misalignment of a channel plate is approximately the transverse displacement of one end of the plate with respect to the other, δ, divided by the length of the plate. δ is selected from a uniform distribution between $\pm\delta_{\max}$. Because no reliable mea-

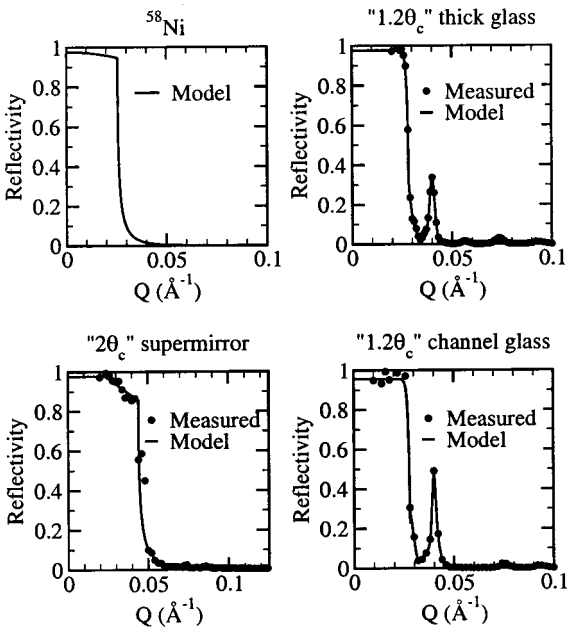

FIG. 3. Measured reflectivities (symbols) and modeled reflectivities (lines) for the DCS neutron guide system, plotted as a function of the wave-vector transfer, Q. These correspond to (clockwise from top left) ^{58}Ni, ^{58}Ni-equivalent coating on polished glass, ^{58}Ni-equivalent coating on float glass, and $2\theta_c$ supermirror, where θ_c is the reference critical angle of natural nickel.

surement of the maximum plate–groove clearance is available, we have estimated it by performing simulations with different choices of $\delta_{\max}$.

Consistent with the conclusions of Allenspach *et al.*,[6] the effect of the transverse displacements of the plates on reducing the effective cross-sectional areas of the channels is estimated to be no worse than the effect of increasing the channel separator thickness from 1 mm to 1 mm$+\delta_{\max}$. (This at least gives the worst case for a perfectly collimated beam.) Thus the reduction of the transmission due to this effect is estimated to be no more than about 4.5% and probably significantly less. Because these effects are small, like the vertical misalignments, we have also chosen to ignore them in this model. Consequently, the refined value of $\delta_{\max}$ is expected to absorb the effects of the vertical misalignments and cross-sectional area differences that are present in the real guide. This means that the refined value of $\delta_{\max}$ is expected to be slightly larger than the actual maximum plate–groove clearance.

Figure 3 shows examples of the model reflectivities, $R(Q)$ (lines), plotted as a function of the wave-vector transfer, Q, that were used to simulate each type of coating represented in the DCS neutron guide. Where available, the modeled curves were based on measured reflectivity data[11] (shown by symbols). The ^{58}Ni coatings shown in Fig. 3 apply to in-pile sections of the guide. The measurements for the ^{58}Ni-equivalent coatings reveal Bragg scattering at $Q \approx 0.04\,\text{Å}^{-1}$. This is because the thickness of most of the bilayers is uniform, giving rise to a pronounced Bragg peak beyond the critical cutoff angle for total reflection. The lines show that this is accounted for in the modeled reflectivities. In the supermirror this structure is almost absent because such coatings are produced with graduated layer thicknesses that produce a quasicontinuum of Bragg peaks beyond the ordinary critical angle, thus effectively extending it. For all reflectivity models based on measured data, the model curve is multiplied by a variable, R_0, which corresponds to $R(Q \rightarrow 0)$, the reflectivity at grazing incidence. The value of R_0 was refined to best reproduce the magnitudes and features of the measured data described in Sec. III. For the ^{58}Ni coatings, the models are analytical functions developed from measurements on ^{58}Ni guide systems elsewhere at the NCNR. Their model parameters were not refined for these calculations.

V. CHOPPER TRANSMISSION

In order to compare calculated and measured integral fluxes with the choppers turning, we must account for the chopper slot transmissions. Given in Ref. 12 are analytical expressions for the chopper transmission for counterrotating, radially shaped slots illuminated by rectangular guide channels, assuming perfect disk phasing and negligible counterrotating disk separation. Each channel i, which may or may not be centered horizontally with respect to the center of the slot opening, is assumed to have spatially uniform flux of magnitude ϕ_i. The number of neutrons transmitted through a slot pair per pulse due to channel i is just the integral of a function $A^i(t)$ over one slot opening period, τ, multiplied by the respective mean channel flux, ϕ_i. $A^i(t)$ represents the area of channel i that is viewable through the slots at a given instant, t. The number of neutrons transmitted per pulse is just the sum of the integrals,

$$\sum_i \phi_i \int_0^\tau A^i(t)dt,$$

where the sum runs over all channels i. For radially shaped slots and rectangular channel cross sections, these integrals are analytical and fully account for the nonzero channel separator thicknesses. It was also shown[12] that the number of neutrons per pulse with the choppers phased to select a wavelength λ_0 is given approximately by

$$N_{\text{pulse}}(\lambda_0) = \frac{h}{m_n L_{PM}} \sum_{i=1}^{n_{\text{ch}}} \frac{1}{A_0^i} \left(\frac{d\phi(\lambda_0)}{d\lambda} \right)_i \times \int_0^{\tau_P} A_P^i(t_P)dt_P \int_0^{\tau_M} A_M^i(t_M)dt_M, \quad (1)$$

where n_{ch} is the number of channels in the guide, $A_P^i(t_P)$ and $A_M^i(t_M)$ are the areas of channel i that are viewable at time t_P through the pulsing disk slots and at time t_M through the monochromating disk slots, respectively, L_{PM} is the mean separation of the pulsing and monochromating disk pairs, A_0^i is the cross-sectional area of channel i, m_n is the neutron mass, and h is the Planck constant. The terms $(d\phi(\lambda_0)/d\lambda)_i$ represent the neutron current density per unit wavelength λ in channel i (evaluated at λ_0) at the exit of the bare chopper guide (without the chopper disks but including corrections for the transmission of the guide windows, chopper slot ma-

terial, and other semitransparent materials in the beam). These differential fluxes were obtained from the Monte Carlo simulations of the guide.

Finally, the time-averaged neutron current density delivered by the chopper system with all disks turning is just $N_{\mathrm{pulse}}(\lambda_0)$ multiplied by the number of pulses per second, divided by the beam area over which the flux is to be averaged. For a fair comparison with the measured fluxes, the outer envelope area of the transmitted beam was used for the flux averaging. For the five-channel guide these areas are about 29.5, 14.0, and 4.9 cm^2 for the low, medium, and high resolution modes, respectively. Qualitatively, the counterrotating slots favorably bias transmission of neutrons traveling closest to the horizontal center of the guide where the slots are open the longest. Therefore increasing the neutron intensity at the center of the guide is more profitable for increasing the instrumental intensity than on the edges.

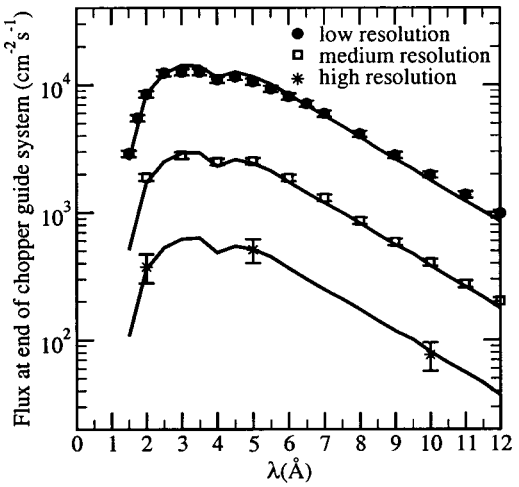

FIG. 4. Comparison of measured beam fluxes at the beam monitor position in the three resolution modes (symbols) with the corresponding simulated fluxes (lines). These comparisons were made for all chopper disks running at 20 000 rpm. Note that these flux measurements were made prior to installation of the graphite beam filter (January 2001) and the higher intensity liquid hydrogen cold source (March 2002).

VI. SIMULATIONS

A. Simulations of the original five-channel chopper guide

Monte Carlo simulations of the original five-channel chopper guide were performed in an effort to reproduce as closely as possible the neutron fluxes, flux ratios, and spectral shapes obtained from the measurements outlined in Sec. III. The simulation method described in Ref. 6 generates random Gaussian misorientations of the reflecting surface at each reflection, thus simulating the average behavior of many guides with the same misorientation probability distributions. In contrast, we simulate fixed misalignment configurations of the plates, such that the surface misorientation experienced by a neutron impinging on a particular channel plate is always the same. By changing the random seed, different random configurations of the glass plates were explored using the same misalignment probability distributions. The resulting simulation values of $(d\phi/d\lambda)_i$ for each channel i, were inserted into Eq. (1) when comparing with measurements carried out with the choppers turning. Although more laborious, this method quickly revealed typical ranges of transmissions that could be expected for given values of $\delta_{\max}$ and R_0. We found that the spectral distributions cannot be satisfactorily reproduced at short wavelengths for any reasonable value of R_0 until $\delta_{\max}$ reaches about 0.3 mm (our estimated upper limit). Once this was established, we fixed $\delta_{\max}$ at 0.3 mm and explored different misalignment configurations. Having found reasonable agreement between the measured and simulated short wavelength spectra (the latter revealing itself to be much more sensitive to the specific misalignment configuration than to parameter R_0 within its reasonable limits), the random seed was frozen to preserve specific misalignments of the plates. Then, parameter R_0 was refined until a good description of the spectrum was achieved over the entire wavelength range. After several fine-tuning iterations of this process, a model configuration was found that reproduced the measured fluxes, their ratios, and their distributions very well. Figure 4 shows a comparison of early spectrum measurements with the best model predictions evaluated for all chopper disks spinning at 20 000 rpm. Note that these measurements and simulations were performed prior to the introduction of a cooled graphite beam filter in January 2001 and upgrade to a higher intensity cold source in March 2002.[13,14] The good agreement between the simulations and the measurement in Fig. 4 is achieved with $R_0 = 0.96$ for the channel plate coatings. A value of $R_0 = 0.977$ was used for all ^{58}Ni-equivalent coatings on superpolished glass surfaces. The latter value was justified on the basis that it gave excellent agreement between simulated and measured integral fluxes at points upstream of the chopper guide where there are no channels and the superpolished sides and rules have essentially identical coatings to the sides and the rules of the channeled section (excluding the short in-pile section). All the reflectivity models (lines) shown in Fig. 3 are drawn with the refined values of R_0 that evolved from the best-fit simulations.

We discuss now some potential implications of the simulated guide properties on the guide transmission efficiency before discussing possible solutions. If we ignore misalignments for the moment and consider only the reflectivities, we can already say something about an *upper limit* on the channel transmission efficiency. For convenience, we make here a distinction between what we call ''reflectivity losses'' meaning losses from reflections *below* the critical angle due to a mean value of $R<1$ as opposed to ''misalignment losses'' where the neutrons encounter a lowered reflection probability by virtue of the misorientation of the reflecting surface. The most dramatic manifestation of a misalignment loss is the heavy suppression of an angular band of neutrons for which the reflecting surface misalignment alone causes their incident angles to exceed the critical angle, where the reflection probability drops dramatically.

Considering the channels as straight guides of length L, width W, and height H, we may approximate the channel transmission, T, as

$$T \approx F_{\mathrm{LOS}} + (1 - F_{\mathrm{LOS}}) R_x^{\langle N_x \rangle} R_y^{\langle N_y \rangle}, \tag{2}$$

where x denotes values appropriate to the sides of the channel and y denotes the rules, R is the mean reflectivity below the critical angle, and $\langle N\rangle$ is the mean number of reflections. F_{LOS} is the line-of-sight fraction of neutrons and we have assumed that there is negligible absorption or scattering of these neutrons. F_{LOS} can also be written as a product of a side and a rule term, i.e.,

$$F_{\mathrm{LOS}}=F_x F_y, \tag{3}$$

where

$$F_x=\frac{W}{2Lv_c^x(\lambda)}, \quad \theta_c^x(\lambda)\geqslant\frac{W}{L},$$
$$F_x=\frac{2W-\theta_c^x(\lambda)L}{2W}, \quad \theta_c^x(\lambda)<\frac{W}{L}. \tag{4}$$

Likewise,

$$F_y=\frac{H}{2L\theta_c^y(\lambda)}, \quad \theta_c^y(\lambda)\geqslant\frac{H}{L},$$
$$F_y=\frac{2H-\theta_c^y(\lambda)L}{2H}, \quad \theta_c^y(\lambda)<\frac{H}{L}. \tag{5}$$

An expression for the mean number of reflections in two dimensions, $\langle N\rangle$, averaged over all possible trajectories has been given by Mildner,[15] where

$$\langle N\rangle=\frac{\lambda^2}{\lambda^2+\lambda_c^2}, \quad \lambda\leqslant\lambda_c \tag{6}$$

and

$$\langle N\rangle=\frac{\lambda}{2\lambda_c}, \quad \lambda>\lambda_c, \tag{7}$$

where $\langle N_x\rangle$ and $\langle N_y\rangle$ are produced by substituting $\lambda_c=W/(\gamma_x L)$ and $H/(\gamma_y L)$ into the above expressions, respectively, with $\gamma_{x,y}=\theta_c^{x,y}(\lambda)/\lambda$.

For the original guide, we use $R_x=R_0=0.96$ for the channels that are not bounded by a polished glass side wall, $R_x=0.969(=[0.96+0.977]/2)$ for the 6.5 mm outer channels. For R_y we use the mean value $R=0.948$ for the $m=2$ supermirror for $Q\leqslant 0.044\ \text{Å}^{-1}$. We also use $W=4$, 5, or 6.5 mm, $H=100$ mm, $\gamma_x=2.047\times10^{-3}$ rad Å^{-1}, and $\gamma_y=3.463\times10^{-3}$ rad Å^{-1}. We find that the transmission, T, at a typical incident wavelength of 5 Å is about 60% in the 4 mm channel, 66% in the 5 mm channel, and 77% in the 6.5 mm channel. The corresponding values at an incident wavelength of 12 Å are about 29%, 37%, and 53%, respectively. These results strongly suggest that the reflectivity losses alone are costly, especially at long wavelength and that increases of the channel width could significantly reduce these losses.

The above expressions for $\langle N\rangle$ work remarkably well for the channeled guide. For example, for $\lambda>\lambda_c$, the mean number of *side* reflections for the transmitted neutrons obtained from the Monte Carlo is fitted well by $\langle N\rangle\approx 9.2\lambda\ (\text{Å})/W\ (\text{mm})$ for $W=4-15$ mm. This is very close to the value given by Eq. 7 with $\gamma_c=2.047\times10^{-3}$ rad Å^{-1}.

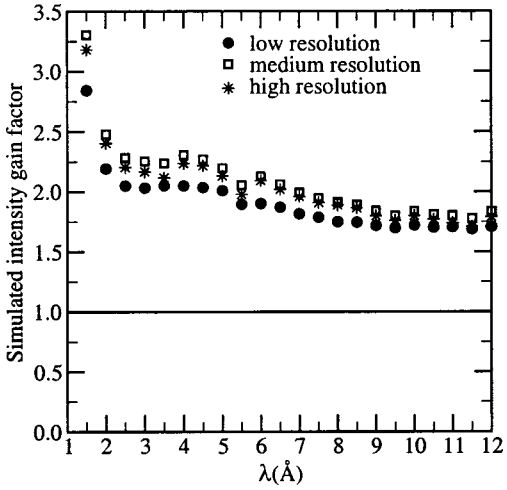

FIG. 5. Simulated monochromatic intensity gain factors for an idealized five-channel replacement guide (perfectly aligned, with reflectivities characterized by $R_0=0.99$) compared with those for the original five-channel guide configuration. The gain factors are averages over the envelope of the transmitted beam.

It is clear that the plate misalignments have a significant and complex influence on the channel transmission at short wavelengths. The misalignments also cause measurable losses in the transmission at the longer wavelengths but the loss factor is less wavelength dependent.

B. Simulations of an optimum performance five-channel guide

An obvious option for increasing the beam intensity is to replace the original five-channeled guide with one that has improved plate alignment and reflectivity. One construction method that potentially increases the channel plate alignment by an order of magnitude is to sandwich the plates between parallel spacers that also serve as the rules. In order to make a realistic estimate of the maximum intensity increases expected for this option, we performed simulations for the five-channeled guide in which the plates and sides are perfectly aligned with all coatings characterized by $R_0=0.99$. This figure is judged to represent the maximum value achievable for this type of coating using current technology. Figure 5 shows the anticipated maximum intensity gain factors that could be expected if the original guide were replaced with this optimal five-channel guide. If we estimate the transmission in this case, as described in Sec. VI A, we find T at 5 Å is about 86% for the 4 mm channels, 88% for the 5 mm channel, and 90% for the 6.5 mm channels. The corresponding values at an incident wavelength of 12 Å are about 69%, 73%, and 76%, respectively, a significant improvement.

C. Simulations of a modified guide

Replacing the five-channeled guide is relatively expensive and carries the additional risk that the performance may fall substantially short of the assumed upper-limiting case described in Sec. VI B. Therefore, we investigated an alternative option in which the existing guide is modified in an effort to increase the intensity by reducing the number of reflections and their associated loss. The simplest option

available that is most likely to achieve the desired effect consists of removing the two innermost channel separators, thereby creating a three-channel guide with (nominally unchanged) 6.5 mm width outer channels and a center 15 mm wide channel. This configuration is expected to especially benefit the low and medium resolution mode intensities because the existence of the center channel of the five-channel guide benefits only the high resolution mode at the expense of some low and medium resolution mode intensity. The potential gains for the low and medium resolution modes are threefold: (i) the losses in the widened center channel are reduced by decreasing the number of neutron contacts with the channel walls, (ii) the beam area viewable through the wide and medium width slots is increased by 200 mm^2, due to the removal of the two inner 1 mm wide$\times$100 mm tall separators, and (iii) the counterrotating chopper slots are open longest at the horizontal bisector of the guide where the significant guide flux increases are achieved. This means that the intensity gain factors with the choppers turning are greater than the guide transmission gain factors alone.

In order to quantify the gains for the three-channel guide, the two remaining channel separators were modeled using $R_0=0.96$ and $\delta_{\max}=0.3$ mm, exactly as they were in the best-fit model of the original five-channel guide (see Sec. VI A). The resulting transmission is not surprisingly less sensitive to the specific plate misalignment configuration because (i) the number of neutron contacts in the center 15 mm wide channel is reduced by roughly a factor of 3 compared to the 4 and 5 mm width channels previously, and (ii) the line-of-sight fraction of neutrons in the center channel is increased by about a factor of 3. Repeating our instructive estimates of T (ignoring misalignments) with $R=R_0=0.96$ for the 15 mm channel and $R=0.969$ for the 6.5 mm outer channels, the values of T at 5 Å are about 85% in the 15 mm center channel and 77% in the outer 6.5 mm channels. The corresponding values at 12 Å are about 67% and 53%, respectively. In comparing values of T, we conclude that the three-channel guide might have similar intensity to the optimum five-channel guide near the horizontal center of the beam where intensity counts the most, with the added bonus that the former has two less channel separators blocking the beam.

In the case of the three-channel guide, the smaller values of $\langle N\rangle$ in the widened center channel improve the transmission rather than the larger values of R in the optimum five-channel case. Nonetheless, a detailed analysis that accounts correctly for misalignments and the presence or absence of channel separators is best handled by the Monte Carlo simulations. The simulated intensity gain factors for the modified guide with respect to the original five-channel guide are shown in Fig. 6. The data shown by symbols were produced using the specific plate misalignments that best describe the original five-channel guide transmission. The shaded bands indicate ranges of gain factors obtained from 10 additional random arrangements with the same values of $\delta_{\max}$ ($\delta_{\max}=0.3$ mm) and R_0. These bands are considered to be representative of the statistical spread of gain factors that might be observed once the channel plates are jogged from their initial positions. (This is considered to be almost inevitable when removing the inner channel separator plates, which requires complete removal of the guide sections.) For comparison, the solid, dashed, and dotted lines are simulated gain factors obtained for the low, medium, and high resolution modes with the channel plates *perfectly aligned* in both configurations.

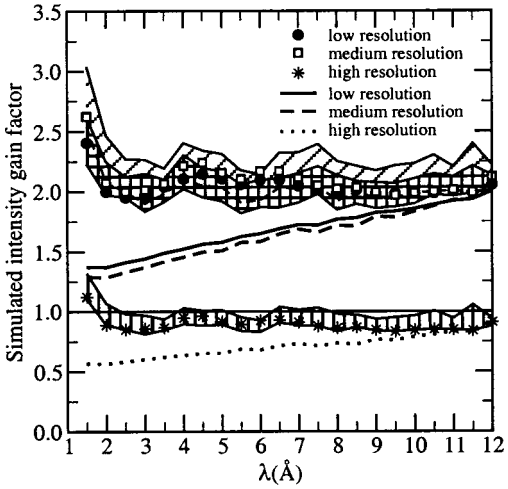

FIG. 6. Simulated monochromatic intensity gain factors for the three-channel guide configuration compared with those for the original five-channel guide configuration. The gain factors are averages over the envelope of the transmitted beam. The data shown by symbols were produced using a plate misalignment distribution that best explains the collective five-channel flux measurements. The shaded bands indicate predicted ranges of gain factors obtained from 10 other random arrangements of the plates from the same plate misalignment probability distribution. Cross hatched, slanted hatched (partially occluded), and vertically hatched regions represent calculations for the low, medium, and high resolution modes, respectively. The solid, dashed, and dotted lines are the corresponding predicted gain factors with the misalignments "switched off" (i.e., perfectly aligned).

The simulated intensity gain factors for the three-channel guide with respect to the optimum five-channel guide are shown in Fig. 7. This figure indicates that the three-channel guide should outperform the optimum five-

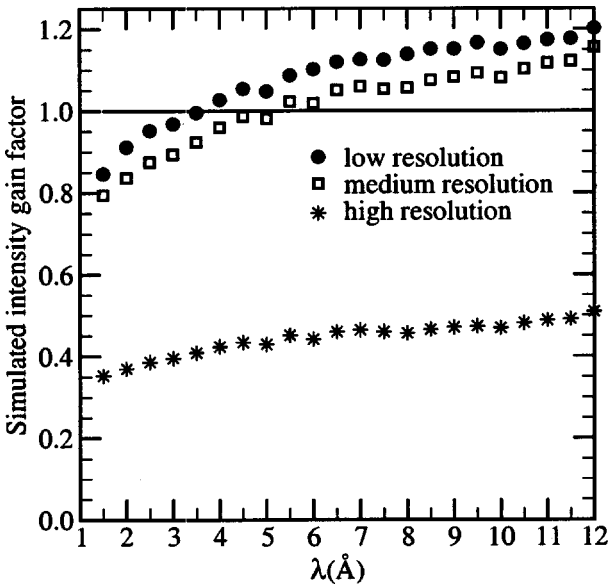

FIG. 7. Simulated intensity gain factors for the modified three-channel guide with respect to the optimum five-channel guide for the three resolution modes.

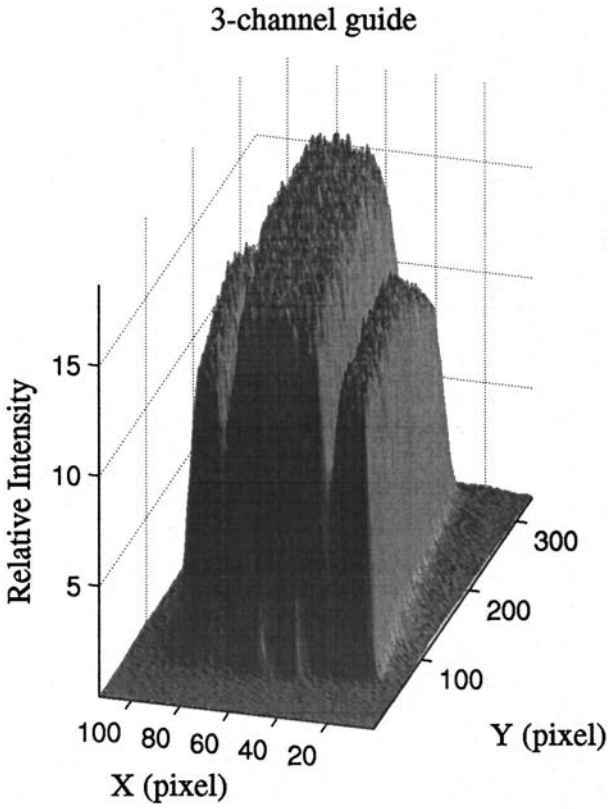

FIG. 8. Measured spatial distribution of neutron flux at the end of the three-channel guide. In contrast with the measurement shown in Fig. 2, which was performed with the chopper disks removed, this measurement was performed with all but the first pulsing chopper disk stopped with the widest slots of the stationary choppers aligned in the beam. The falloff of intensity near the top of the outer channels (not seen in Fig. 2) results from partial eclipse of this part of the guide by the widest monochromating slots (see Fig. 1). This falloff would disappear if the chopper disks were removed.

channel guide for all wavelengths above about 5 Å for the low and medium resolution modes. However, for the high resolution mode, the idealized five-channel guide is expected to be two to three times better.

In light of the usage trends of the DCS, the modification of the guide to the proposed three-channel arrangement was deemed to be the most cost-effective and indeed favorable solution for the majority of experiments. Conversion to the three-channel arrangement was undertaken in July 2002.

VII. MEASUREMENTS OF MODIFIED GUIDE PERFORMANCE

Following guide modification, the beam profile was remeasured with a Dy foil. This measurement was performed with all but one of the chopper disks stopped with their widest slots aligned in the beam. The result is shown in Fig. 8. The vertical scale is arbitrary but the transmission of the outer channels is approximately the same as before; small differences can occur because of rearrangement of the channel plates in their grooves. A comparison of Fig. 8 with Fig. 2 clearly shows the flux enhancement in the center portion of the beam.

Figure 9 shows the measured beam area-averaged intensity gains for the three chopper resolution modes measured with the chopper disks spinning at 20 000 rpm. The increased

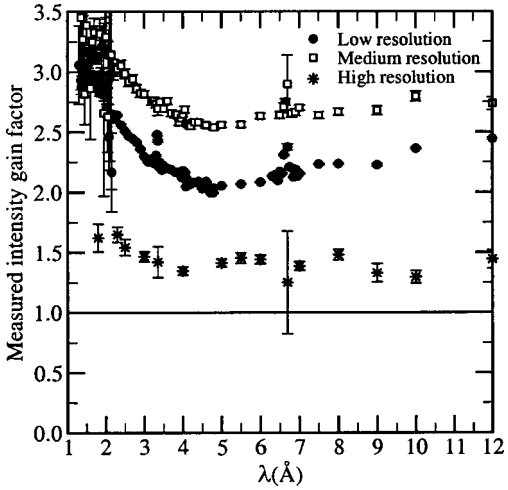

FIG. 9. Measured intensity gains as a function of the wavelength derived from before and after incident beam monitor measurements for the three-channel guide relative to the those for original five-channel guide.

uncertainties at $\lambda = 3.35$ and 6.7 Å are associated with reduced counting statistics at these wavelengths because of sharp dips in the beam intensity caused by the (004) and (002) Bragg peaks of the graphite filter (installed upstream of the chopper system). The significant structure in the filter transmission at wavelengths below about 2.2 Å is also responsible for the fluctuating uncertainties there. A comparison of these results with the predicted gains shown in Fig. 6 reveals that the measured gains exceed expectations for all three resolution modes.

The most significant disagreement between the simulations and the measurements occurs for the high resolution mode where the simulations predict barely a break-even gain factor while the measured gains are typically between about 30% and 40%.

VIII. DISCUSSION

We see from Fig. 9 that the measured gain factors in all three resolution modes have the same characteristic wavelength dependence, a tendency to rise sharply at short wavelength, with a fairly wavelength-independent portion at intermediate wavelength, and a tendency to drift upward at long wavelengths. This general trend is observed in the simulation results for all the different configurations of glass plates investigated (see the curves for misaligned plates in Fig. 6). By comparing the simulated intensity gain curves for the aligned and misaligned channels in Fig. 6, we see that the gains appear to be driven mainly by the reflectivity losses at long wavelength where the two gain factors are similar. Furthermore, in the absence of misalignments, the gain factor for the three-channel guide compared with the five-channel guide tends to continuously increase with an increase in wavelength in the wavelength range from about 2 to 12 Å.

We can easily crosscheck the trends indicated by the simulation results for the aligned case relative to those obtained from the analytical model for perfectly aligned channels described in Sec. VI A. We calculate the transmission, T_i, [using Eq. (2)] for each channel i and substitute the resulting values into Eq. (1) in place of the terms $(d\phi/d\lambda)_i$.

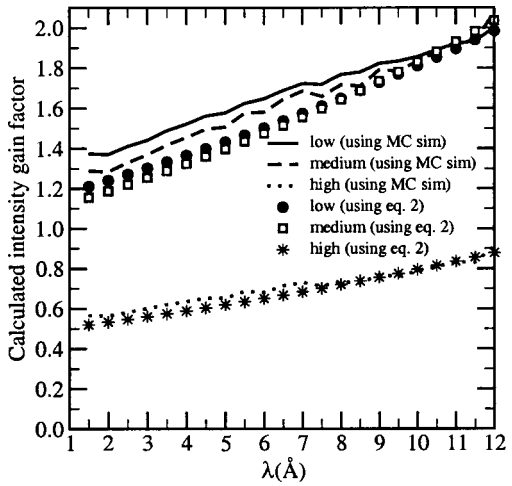

FIG. 10. Predicted intensity gain factors for the modified three-channel guide compared with the original five-channel guide assuming that both are perfectly aligned. Two calculation methods are compared. The solid, dashed, and dotted lines are the gain factors obtained using Monte Carlo simulation (also shown in Fig. 6) for the low, medium, and high resolution modes, respectively, using the detailed model reflectivity curves. The circles, open squares, and stars are the corresponding gain factors obtained using Eqs. (2) and (1) with the parameters given in the example in Sec. VI Å, i.e., $R_x = 0.969$ (outer channels), $R_x = 0.96$ (inner channels), $R_y = 0.948$, $\gamma_x = 2.047 \times 10^{-3}$ rad/Å, and $\gamma_y = 3.463 \times 10^{-3}$ rad/Å.

By taking the ratio of the quantities given by Eq. (1) for the three-channel case and the five-channel case, so that the source spectrum-dependent quantities cancel one another, we obtain the analytical gain factors. Figure 10 shows a comparison of the gain factors obtained using the Monte Carlo results (also shown in Fig. 6) for each of the aligned cases with the gain factors obtained by the analytical technique. The values of the parameters used in the latter case are identical to those described in Sec. VI A. The agreement between the two techniques is remarkably good and provides little evidence of the short wavelength upturn of the gain factors observed in the measurements and in the simulations when misalignments are included. We therefore attribute the short wavelength trend to the effect of misalignment of the glass plates.

Naively, one might expect the gain factor due to plate misalignment to be roughly independent of the wavelength. If α represents the mean misalignment of plates that are oriented such that they *decrease* the reflection probability, the ratio $\alpha/\theta_c(\lambda)$ varies inversely proportional to λ. On the other hand, at least for $\lambda > \lambda_c$, the number of times that the mean trajectory encounters the plates increases roughly proportionally to λ, so the two effects tend to cancel one another. However, there are cases where clearly this argument breaks down; for example, when $\alpha \gg \theta_c(\lambda)$ or when the mean number of neutron contacts with the sides of the channels becomes small, for example, of order one or less. Both of these situations can occur for an increasing fraction of trajectories as $\lambda \to 0$.

Perhaps a qualitative explanation can be illustrated in terms of the familiar behavior of a uniformly illuminated bent guide with no line of sight. The transmission of such guides is characterized by a short-wavelength ''cutoff,'' which is the maximum wavelength for which all trajectories impinging on the bend have incident angles that exceed the critical angle. For a simple ''V'' bend with bend angle β, the cutoff is at a wavelength for which the critical angle is $\beta/2$. As the wavelength increases above the cutoff wavelength an increasing fraction of trajectories reflect, resulting in a progressive increase in the transmission. As the wavelength increases further, a maximum in the transmission may be reached (at $\lambda = \lambda_{pk}$), beyond which the transmission falls at longer wavelengths because the increased number of contacts with the guide walls results in greater reflectivity loss. In the misaligned channel, if we consider α the analog of the bend angle β, we might expect the transmission characteristics of the neutrons *that encounter the channel walls* to be similar to those of the bend. However, because a line of sight is present, there is no complete cutoff. If the bent guide is widened, proportionately more trajectories have a line of sight and fewer undergo reflection. Typically, when comparing the wider bent guide to the narrower one, this results in a gain factor that increases as the wavelength decreases below λ_{pk}. This is because the cutoff behavior associated with contact with the sides affects a smaller fraction of neutrons in the wider guide and in such a way that this fraction decreases faster with a decrease in wavelength than in the narrower guide. The long wavelength increase of the gain factor is attributed to the apparent dominance of reflectivity loss at these wavelengths. The reduced mean number of reflections in the wider guide relative to that in the narrower guide gives rise to smaller exponents in Eq. (2) for the former and hence a gain factor that increases with increasing wavelength.

Although useful approximations to the transmission of simple geometry bent and curved guide systems can be obtained with non-numerical methods,[16,17] in complicated situations with many independently oriented reflecting surfaces and lines of sight, calculation of the transmission is best handled by Monte Carlo methods. We have used the illustration of the bent guide only to demonstrate the plausibility of the Monte Carlo results.

We turn now to the apparently poor reflectivity of the coatings on the channel separators. Float glass has tended to be the preferred substrate for short devices with multilayer or supermirror coatings because the root mean square (rms) surface roughness can be nearly an order of magnitude better than that of mechanically polished glasses; typically 3–4 Å is possible.[7] Low roughness is particularly desirable for multilayers because the substrate roughness tends to be reproduced in the layer boundaries and amplified as increasing numbers of layers are deposited. Senthil Kumar *et al.*[18] reported that one technique that greatly reduces cumulative buildup of interfacial roughness in successive layers is ''reactive sputtering.'' However this technique has not been observed to lower the minimum roughness of the interfaces and therefore good reflectivity relies on smooth substrates. Typically a rms roughness of about 5 Å or less is required for layer thicknesses of 50 Å.[7] (To make a ^{58}Ni-equivalent coating, typically bilayer thicknesses in the range of about 240–290 Å are necessary). Despite its low roughness, float glass can be difficult to produce with acceptable flatness (i.e., the degree of variation of the slope of the surface). Typically flatness of 10^{-4} rad or less is required over length scales of

the order of 0.5 m.[7] Slope variations of excessive amplitude can be problematic for short wavelengths where the surface normal variation is a non-negligible fraction of the critical angle, or for long devices where many reflections may be required for transmission. Majkrzak and Ankner[19] have also noted that great difficulty has been encountered in the production of Ni–Ti multilayers with low interface roughness and that large roughness reduces the specular scattering power and increases the off-specular diffuse and multiple scattering of the layers. They pointed out that more amorphous, smaller grain size layers of lower interfacial roughness have been produced by alloying the nickel with carbon and the titanium with manganese. We speculate that the combination of insufficient flatness of float glass substrates and high intrinsic interfacial roughness of Ni–Ti bilayers might be the origin of the poor average performance of channel separator plates.

ACKNOWLEDGMENTS

The authors are grateful to the National Science Foundation for financial support under Agreement No. DMR-0086210. They express their sincere gratitude to the NIST staff who were involved in this project, in particular, George Baltic, Yu-Tarng Cheng, Dave Clem, Doug Johnson, Doris Kendig, Dick Lindstrom, Don Pierce, Mike Rinehart, Sushil Satija, and Scott Slifer. They are especially indebted to Craig Brown for his useful comments and suggestions and to David Mildner for providing invaluable insights and suggestions.

APPENDIX: RELATIVE IMPORTANCE OF HORIZONTAL AND VERTICAL MISALIGNMENTS FOR THE DCS CHANNELED GUIDE

Suppose that the attenuating effect of the misalignments scales roughly proportionally to the number of reflections, N, multiplied by the mean absolute misalignment angle, α, divided by the critical angle, θ_c. In this case, N is approximately proportional to θ_c/W in the horizontal and θ_c/H in the vertical, where W and H are the width and height of the guide, respectively. The mean magnitude misalignment angle, α, is approximately $\langle|\delta|\rangle/L$ in the horizontal and $\langle|\delta|\rangle/H$ in the vertical, where L is the length of the misaligned guide and $\langle|\delta|\rangle=\delta_{\max}/2$ is typical of the transverse displacement of one end of the guide with respect to the other (assumed to be the same horizontal and vertical). Therefore, we might expect that the ratio of the importance of the horizontal to vertical misalignments, κ, varies roughly as $\kappa\approx H^2/LW$. For $H=100\,\text{mm}$, $W\approx 5\,\text{mm}$, and $L\leqslant 250\,\text{mm}$, we have $\kappa\geqslant 8$.

[1] J. R. D. Copley and J. C. Cook, Chem. Phys. **292**, 477 (2003).
[2] J. R. D. Copley, Nucl. Instrum. Methods Phys. Res. A **303**, 332 (1991).
[3] J. R. D. Copley, Physica B **180 & 181**, 914 (1992).
[4] R. E. Lechner, *Neutron Scattering in the Nineties* (IAEA, Vienna, 1985), p. 401.
[5] J. R. D. Copley, Nucl. Instrum. Methods Phys. Res. A **291**, 519 (1990).
[6] P. Allenspach, P. Böni, and K. Lefmann, Proc. SPIE **4509**, 157 (2001).
[7] F. Samuel, B. Farnoux, B. Ballot, and B. Vidal, Proc. SPIE **1738**, 54 (1992).
[8] W.-T. Lee and F. Klose, Proc. SPIE **4509**, 145 (2001).
[9] Y.-T. Cheng, radiograph measurements, NIST (unpublished).
[10] R. Lindstrom, activation results, NCNR (unpublished).
[11] S. Satija, reflectivity measurements, NCNR (unpublished).
[12] J. C. Cook, NCNR internal report (2001).
[13] R. E. Williams and J. M. Rowe, Physica B **311**, 117 (2002).
[14] R. E. Williams, P. Kopetka, J. C. Cook, and J. M. Rowe, Proceedings of the 9th Meeting of the International Group on Research Reactors (IGORR-9), Sydney, Australia, 2003, http://www-igorr.cea.fr/proceedings/igorr9/papers/sns_04.pdf
[15] D. F. R. Mildner, Nucl. Instrum. Methods Phys. Res. A **292**, 693 (1990).
[16] D. F. R. Mildner, Nucl. Instrum. Methods Phys. Res. A **290**, 189 (1990).
[17] J. R. D. Copley, J. Neutron Res. **2**, 95 (1994).
[18] M. Senthil Kumar, P. Böni, and D. Clemens, Physica B **276–278**, 142 (2000).
[19] C. F. Majkrzak and J. F. Ankner, Proc. SPIE **1738**, 150 (1992).